REACTIVE POWER ADEQUACY IN DISTRIBUTION NETWORKS WITH EMBEDDED DISTRIBUTED ENERGY RESOURCES[1]

F. Milano[2], A. J. Conejo[3], and J. L. García-Dornelas[4]

ABSTRACT

This paper addresses reactive power adequacy problems in distribution networks that include a significant number of distributed energy resources. The voltage profile of the distribution network is analyzed under increasing amounts of generation provided by the distributed energy resources. Both static and dynamic voltage disruption phenomena resulting from increasing distributed generation are described and the need for remedial actions identified. Different reactive power control schemes are then proposed to keep both an appropriate voltage profile and an appropriate voltage stability margin. Finally, an economic appraisal of remedial actions is carried out and the responsible parties identified. Results from a realistic case study are presented and discussed. Conclusions are duly drawn.

CE Database Subject Headings: distributed energy resources, distribution network, reactive power adequacy, voltage stability, wind energy.

---

[1]Manuscript # EY22077 presented at the Journal of Energy Engineering, Special Issue on Distributed Energy Resources − Potentials for the Electric Power Industry.

[2]Assistant professor at the Department of Electrical Engineering, University of Castilla-La Mancha, 13071 Ciudad Real, Spain. E-mail: Federico.Milano@uclm.es.

[3]Full professor at the Department of Electrical Engineering, University of Castilla-La Mancha, 13071 Ciudad Real, Spain. E-mail: Antonio.Conejo@uclm.es.

[4]Unión Fenosa Distribución, Avenida Arteixo, 171, 15008 A Coruña, Spain. E-mail: JLGarcia@uef.es.

INTRODUCTION

Motivation

Distributed Energy Resources (DER) for electric energy production are being connected in increasing quantity to weak distribution network in rural areas.

Particularly relevant is the connection to distribution networks of wind farms, which rely on a technology already proved as profitable. Wind power penetration is indeed very significant in different countries around the world (DeMeo et al. 2005; Eriksen et al. 2005; Zavadil et al. 2005), including off-shore developments (Pool 2005).

This increasing amount of DERs embedded in weak distribution networks results more often than not in voltage problems due to the unavailability of appropriate reactive power resources and fast enough control schemes.

Problem Description

Increasing production of electric energy from DERs within a distribution network results in diminishing energy flows from the feeding substations to the demands (substation-to-demand flows) that are located throughout the network.

These substation-to-demands flows eventually revert their directions provided that the DER energy production increases sufficiently to convert the distribution network into a net exporter of energy.

This paper considers both static and dynamic voltage and reactive power problems in the distribution network related to the decrement in the feeding flows from the substations that eventually revert their directions.

Analysis and Solutions

Four studies are carried out to comprehend voltage behavior as feeding flows decrease and revert directions. From these four cases, voltage profiles and voltage stability margins are comprehensively analyzed. These cases are briefly described below:

1. Constant power factor. In this operation mode each DER maintains the power factor of its corresponding injection bus close to one. In particular, close to full capacity, wind farms are typically operated with power factor about 0.96. This is actually the policy used by wind farms in mainland Spain, although the Spanish regulation only imposes that the power factor is over 0.86 (B.O.E. 219 1985).
2. Single Under Load Tap Changer (ULTC). In this operation mode each DER maintains the power factor of its corresponding injection bus close to one, while the feeding substation is connected to the distribution network through a ULTC that maintains an appropriate voltage profile throughout the distribution network.
3. Constant voltage magnitude. In this operation mode each DER maintains the voltage magnitude of its corresponding injection bus close to a pre-specified target value close to one.
4. Several Static VAr Compensators (SVCs). In this operation scheme each DER contributes in a coordinate manner to maintain an appropriate voltage profile throughout the distribution network using a set of SVCs strategically installed throughout the network.

Literature Review and Contributions

The literature review below focuses on wind power as wind generators are the most common and most cost effective DERs available.

The first issue in wind power studies is to set up a reliable and complete wind turbine model. There are basically three wind turbine architectures (EWEA 2005):

1. Constant speed wind turbine with squirrel cage induction generator.
2. Variable speed wind turbine with doubly fed induction generator.
3. Variable speed wind turbine with direct drive synchronous generator.

In this paper, only the variable speed wind turbine with doubly fed induction generator is considered as it is the most flexible and most common model used in actual wind farms (Slootweg 2003). Observe that the general conclusions that are drawn in this paper would not change if different wind turbine architectures were considered.

For the static behavior of the wind turbine, well-known power flow PQ or PV generator models are adequate. However, dynamic analysis requires a detailed model of the induction motor, the wind turbine and the regulators of the DER. In this paper we use a simplified fundamental frequency model based on what proposed in (Slootweg et al. 2003) and (Slootweg et al. 2005).

Relevant references on wind turbine controllers are: (Miller et al. 1997) for power control, (Muljadi and Butterfield 2001) for pitch control, and (Fan and Salman 1997) and (Hatziargyriou et al. 1997) for voltage control. Although voltage control is possible, observe that typical DERs are generally operated with constant power factor close to one.

If the wind power penetration is large with respect to the total power generation,

transient stability (Slootweg 2003), fault analysis (Cano-Marín et al. 2004) and short term voltage stability (Fengquan et al. 2005) are relevant phenomena.

Due to the actual trend of increasing wind power penetration in developed countries all around the world, long term voltage stability is more and more an actual issue. (Freitas et al. 2005) focuses on long term voltage stability analysis based on the continuation power flow technique, while (Ha and Saha 2004), (Pálsson et al. 2002) and (Pálsson et al. 2003) discuss wind power penetration in distribution networks.

Within the framework of a distribution network including wind farms, the novel contributions of this paper are:

1. Voltage behavior and voltage stability are characterized as substation-to-load flows decrease and revert directions.
2. Three remedial actions based on an ULTC, local DER voltage control and SVCs to avoid voltage disruption phenomena are described and compared.
3. An economic appraisal that identifies responsible parties is provided.

Paper Organization

The remaining of this paper is organized as stated below.

The following section describes the models of the distribution network, the DERs and the SVCs, explains the analysis performed and the computational tools used, and provides remedial actions.

The section dedicated to the case studies provides a detailed analysis using a realistic distribution network that includes several wind farms. The test system is based on an actual England and Wales network model described in (Greene and Dobson 1998) and

(Hawkins 1996). Results are presented and conclusions duly drawn. This section also provides an economic appraisal identifying responsible parties for voltage disruption.

The final section provides some relevant conclusions.

MODELING, ANALYSIS AND SOLUTIONS

Modeling

The following subsections describe the network, the DER model and the regulators. For remedial actions an ULTC and SVCs are considered. The characteristics of the ULTC and the SVC devices are also described in the final part of this section.

Network Model

A partly meshed rural distribution network that includes one feeding substations is considered for the analysis. The power flow equations of such a distribution system of n buses can be written as follows:

$$P_i = \sum_{k=1}^{n} Y_{ik} v_i v_k \cos(\theta_i - \theta_k - \alpha_{ik}), \quad \forall i = 1, \ldots, n_P \tag{1}$$

$$Q_i = \sum_{k=1}^{n} Y_{ik} v_i v_k \sin(\theta_i - \theta_k - \alpha_{ik}), \quad \forall i = 1, \ldots, n_Q \tag{2}$$

where P_i and Q_i are the active and reactive power injections at bus i, respectively, (Y_{ik}, α_{ik}) are the element (i, k) of the network admittance matrix $\boldsymbol{Y}$, and (v_i, θ_i) and (v_k, θ_k) are the voltages at buses i and k, respectively. The feeding substation is the slack bus of the distribution network. n_P is the number of active power balances, typically $n_P = n - 1$ with single slack bus, and n_Q is the number of buses with unknown voltage magnitudes, i.e. PQ buses and pure transit buses, in the standard power flow problem.

DER Model

DERs in the form of wind generators are located throughout the distribution network. We consider the steady-state electrical equations of the doubly fed induction generator, as the stator and rotor flux dynamics are sufficiently fast in comparison with electromechanical modes and regulator dynamics. Furthermore, the converter controls basically decouple the generator from the grid. As a result of these assumptions, stator (v_{ds}, v_{qs}) and rotor (v_{dr}, v_{qr}) voltages can be expresses as:

$$\begin{aligned} v_{ds} &= -r_S i_{ds} + ((x_S + x_m) i_{qs} + x_m i_{qr}) \\ v_{qs} &= -r_S i_{qs} - ((x_S + x_m) i_{ds} + x_m i_{dr}) \\ v_{dr} &= -r_R i_{dr} + (1 - \omega_m)((x_R + x_m) i_{qr} + x_m i_{qs}) \\ v_{qr} &= -r_R i_{qr} - (1 - \omega_m)((x_R + x_m) i_{dr} + x_m i_{ds}), \end{aligned} \tag{3}$$

where the stator voltages are functions of the grid voltage magnitude v and phase θ at the DER bus:

$$\begin{aligned} v_{ds} &= v \sin(-\theta) \\ v_{qs} &= v \cos(\theta). \end{aligned} \tag{4}$$

In the equations above, r_S is the stator resistance, x_S is the stator reactance, r_R is the rotor resistance, x_R is the rotor reactance, x_m is the magnetizing reactance, ω_m is the rotor speed, $i_{dr} + j i_{qr}$ is the rotor current and $i_{ds} + j i_{qs}$ is the stator current. The active and reactive powers injected (P and Q) into the grid at the DER bus depend on the stator

and rotor currents as follows:

$$\begin{aligned} P &= v_{ds}i_{ds} + v_{qs}i_{qs} + v_{dr}i_{dr} + v_{qr}i_{qr} \\ Q &= -\frac{x_m v i_{dr}}{x_S + x_m} - \frac{v^2}{x_m} \ . \end{aligned} \tag{5}$$

The equations above are obtained assuming a lossless converter model. The generator motion equation is modeled as a single shaft, as it is assumed that the converter controls are able to filter shaft dynamics. Thus one has:

$$\dot{\omega}_m = (T_m - T_e)/2H_m \ , \tag{6}$$

where H_m is the rotor inertia and the electrical torque T_e is approximated as follows:

$$T_e = -\frac{x_m v i_{qr}}{\omega_b(x_S + x_m)} \tag{7}$$

where ω_b is the frequency rate in rad/s and the mechanical torque T_m is:

$$T_m = \frac{P_w}{\omega_m} \tag{8}$$

being P_w the mechanical power extracted from the wind. The latter is a function of the wind speed v_w, the rotor speed ω_m and the pitch angle θ_p. P_w can be approximated as follows:

$$P_w = \frac{\rho}{2} c_p(\xi, \theta_p) A_r v_w^3 \ , \tag{9}$$

in which ρ is the air density, c_p the performance coefficient or power coefficient, ξ the tip speed ratio and A_r the area swept by the rotor. The tip speed ratio ξ is the ratio between

the blade tip speed v_t and the wind upstream the rotor v_w:

$$\xi = \frac{v_t}{v_w} = \eta_{GB}\frac{2R\omega_m}{pv_w} \ . \tag{10}$$

where R is the rotor radius, p is the number of poles and η_{GB} is the gear box ratio. The $c_p(\xi, \theta_p)$ curve is approximated as follows:

$$c_p = 0.22\left(\frac{116}{\xi_i} - 0.4\theta_p - 5\right)e^{-\frac{12.5}{\xi_i}} \tag{11}$$

with

$$\frac{1}{\xi_i} = \frac{1}{\xi + 0.08\theta_p} - \frac{0.035}{\theta_p^3 + 1} \ . \tag{12}$$

Converter dynamics are highly simplified, as they are fast with respect to the electromechanical transients. Thus, the converter is modeled as an ideal current source, where i_{qr} and i_{dr} are state variables and are used for the rotor speed control and the voltage control respectively (see Figs. 1 and 2).

Differential equations for the converter currents are as follows:

$$\begin{aligned} \dot{i}_{qr} &= \left(-\frac{x_s + x_m}{x_m v}P_w^*(\omega_m)/\omega_m - i_{qr}\right)\frac{1}{T_\epsilon} \\ \dot{i}_{dr} &= K_V(v - v_{\text{ref}}) - v/x_m - i_{dr} \end{aligned} \tag{13}$$

where K_V is the gain of the voltage control loop, v_{ref} is the reference voltage, and $P_w^*(\omega_m)$ is the power-speed characteristic which roughly optimizes the wind energy capture and is calculated using the current rotor speed value (see Fig. 3). It is assumed that $P_w^* = 0$ if $\omega_m < 0.5$ p.u. and that $P_w^* = 1$ p.u. if $\omega_m > 1$ p.u. Thus, the rotor speed control

only has effect for sub-synchronous speeds. Both the speed and voltage controls undergo anti-windup limiters in order to avoid converter over-currents.

Currents limits are used to define active and reactive power limits, which are approximated assuming $v \approx 1$, as follows (Slootweg 2003):

$$\begin{aligned} P^{\min} &\approx -\frac{x_m i_{qr}^{\max}}{x_S + x_m} \\ P^{\max} &\approx -\frac{x_m i_{qr}^{\min}}{x_S + x_m} \\ Q^{\min} &\approx -\frac{x_m i_{dr}^{\max}}{x_S + x_m} - \frac{1}{x_S + x_m} \\ Q^{\max} &\approx -\frac{x_m i_{dr}^{\min}}{x_S + x_m} - \frac{1}{x_S + x_m} \ . \end{aligned} \tag{14}$$

Thus DER models incorporate limited voltage control capabilities. Observe that precise active and reactive power limits should be computed depending on the current operating point (Tapia et al. 2001). However these model details are beyond the scope of this paper.

Finally the pitch angle control is illustrated in Fig. 4 and described by the following differential equation:

$$\dot{\theta}_p = (K_p \phi(\omega_m - \omega_{\text{ref}}) - \theta_p)/T_p \ , \tag{15}$$

where K_p and T_p are the gain and the time constant of the pitch control loop, respectively, and ϕ is a function that allows varying the pitch angle set point only if the difference $(\omega_m - \omega_{\text{ref}})$ exceeds a predefined value $\pm\Delta\omega$. The pitch control works only for super-synchronous speeds. An anti-windup limiter locks the pitch angle to $\theta_p = 0$ for sub-synchronous speeds.

ULTC Model

The ULTC is modeled as a π circuit with no magnetizing shunt between nodes k and m. The algebraic equations of the power injections are as follows:

$$\begin{aligned} P_k &= v_k^2(g_{km} + g_{k0}) - v_k v_m(g_{km}\cos\theta_{km} + b_{km}\sin\theta_{km}) \\ Q_k &= -v_k^2(b_{km} + b_{k0}) - v_k v_m(g_{km}\sin\theta_{km} - b_{km}\cos\theta_{km}) \\ P_m &= v_m^2(g_{km} + g_{m0}) - v_k v_m(g_{km}\cos\theta_{km} - b_{km}\sin\theta_{km}) \\ Q_m &= -v_m^2(b_{km} + b_{m0}) + v_k v_m(g_{km}\sin\theta_{km} + b_{km}\cos\theta_{km}) \ , \end{aligned} \tag{16}$$

where $\theta_{km} = \theta_k - \theta_m$; parameters g_{km}, b_{km}, b_{k0} and g_{k0} are functions of the tap ratio m and the transformer resistance r_T and reactance x_T, as follows:

$$\begin{aligned} g_{km} + jb_{km} &= \frac{m}{\overline{z}} \\ g_{k0} + jb_{k0} &= \frac{1-m}{\overline{z}} \\ g_{m0} + jb_{m0} &= \frac{m(m-1)}{\overline{z}} \ , \end{aligned} \tag{17}$$

where $\overline{z} = r_T + jx_T$. Fig. 5 depicts the ULTC control block diagrams. In this papers we use a continuous model for the ULTC control, as follow:

$$\dot{m} = -Hm + K(v_{\text{remote}} - v_{\text{ref}}) \ . \tag{18}$$

where H and K are the integral deviation and the inverse of the time constant, respectively, of the ULTC voltage control loop. The tap ratio m is subjected to an anti-windup limiter.

SVC Model

The regulator is a simple time constant regulator, as depicted in Fig. 6. In this model, a total susceptance b_{SVC} is considered and the following differential equation holds:

$$\dot{b}_{\text{SVC}} = (K_r(v_{\text{ref}} - v) - b_{\text{SVC}})/T_r \ . \tag{19}$$

where K_r and T_r are the gain and the time constant, respectively, of the SVC voltage control loop. The model is completed by the reactive power injected at the SVC node:

$$Q = -b_{\text{SVC}} v^2 \ . \tag{20}$$

The regulator has an anti-windup limiter, thus the susceptance b_{SVC} is locked if one of its limits is reached and the first derivative is set to zero.

Analysis

The analyses carried out in this paper are twofold. Firstly we consider a static analysis based on a Continuation Power Flow (CPF) tool, (Cañizares 2002), which allows identifying the maximum load increment before reaching voltage instability. The static analysis is then analyzed and validated with time domain simulations.

The CPF analysis is basically a series of power flow solutions parametrized with respect to a scalar parameter or *loading margin* λ. The basic idea of CPF analysis is that all load and generation powers increase following a given linear pattern:

$$P_{\lambda i} = \lambda P_i, \quad Q_{\lambda i} = \lambda Q_i \tag{21}$$

In common practice, it is relevant to know how much the system can be loaded before

reaching the maximum loading condition, or the voltage collapse.

The maximum loading condition can be either associated with a saddle-node bifurcation (transmission network maximum loadability), a limit induced bifurcation (generator reactive power limits), or a physical limit (thermal limits of transmission lines, bus voltage limits, etc.).

In this paper we use the basic concepts of the CPF analysis but we assume that the only powers that are increased by the parameter λ are the powers generated by DERs (hereinafter λ is called *DER generation parameter*). This is so mainly for two reasons:

1. Distribution networks where DERs are installed are typically rural systems with dispersed and almost constant loads (at least in the time frame of DERs power variations). The time frame of rural load variations are several minutes to one hour.
2. DERs have a highly unpredictable generation profile, which depends on the season of the year, daily weather conditions and local wind speed. The time frame of power variations of DERs are few seconds to few minutes.

Due to the fast variations of generation power profiles, the static analysis provided by CPF techniques must be accompanied by a dynamic analysis. In this paper we perform time domain simulations to support and discuss results provided by CPF analysis.

To comprehend voltage behavior as substation-to-load feeding flows decrease and revert directions, we solve two initial analysis:

1. No DERs. In this operation mode the feeding substation is generating all the power needed by the loads.

2. Constant power factor. In this operation mode each DER maintains the power factor of its corresponding injection bus close to one. Nowadays this is the most common operation mode of wind farms.

Assuming a well designed distribution network, the first operation mode does not present voltage problems, while the scheme with DERs can potentially lead to voltage problems and eventually to voltage collapse. This depends on the generated power by DERs and the voltage level at the feeding substation. Remedial actions are considered in the next subsection.

Remedial Actions

Three types of remedial actions are considered.

The first solution approach considers a ULTC at the feeding substation while the second solution considers a local voltage regulation at the DER buses. Finally, the third solution scheme considers two SVC devices installed at the weakest buses of the network.

1. Voltage control through ULTC. In this operation scheme, the feeding substation is connected to the distribution network through a ULTC. The ULTC is used to maintain an appropriate voltage profile throughout the distribution network. This is the typical solution adopted so far in distribution networks without DERs.
2. Voltage control through local voltage regulation at DERs. In this operation mode each DER maintains the voltage magnitude of its corresponding injection bus close to a pre-specified target value close to one.
3. Voltage control through SVCs. In this operation scheme each DER contributes in a coordinate manner to maintain an appropriate voltage profile throughout the

distribution network using a strategically installed set of SVCs.

Whether these remedial schemes allow maintaining appropriate static and dynamic reactive power resources throughout the network is discussed in the following section. For the sake of clarity the operation modes discussed in this paper are summarized in Table 1.

CASE STUDIES

This section describes case studies based on a 40-bus test system. All static and dynamic simulations were performed using the software package PSAT (Milano 2005). Further details on models and algorithms used in the simulations are given in (Milano 2002).

Figure 7 depicts a partly meshed 40-bus distribution network, which is considered to carry out diverse case studies. This system is partly based on a simplified model of the Southwest England power system and firstly appeared in (Hawkins 1996). Most power flow data of the test system can be found in (Greene and Dobson 1998) while specific data that refer to DERs and control schemes are provided in the Appendix. The network presents 40 buses, 65 lines and 17 loads for a total load of about 41 MW and 7 MVAr. There are three voltage levels, namely 132, 33 and 11 kV. The feeding substation is located at bus 40 at 132 kV. Buses 20, 22, and 29-37 are at 11 kV, while all remaining buses are at 33 kV. DERs in the form of wind generators are located at buses 6, 13, 18, 20, 22, 24 and 38 (in Fig. 7 static data of DERs are represented by means of a "PQ" within a circle, whereas dynamic data and control parameters are represented by a doubly fed induction motor with a wind turbine). These DERs incorporate fast although limited voltage control capabilities, which are basically related to the rotor current limits of the

machine (Tapia et al. 2001). Furthermore we assume that all DERs have a nominal power of 20 MVA. Observe that DER nominal apparent power limits are never reached in the CPF analyses discussed in the following sections.

In this case study the number and the position of DERs as well as feeding substations are assumed to be fixed. Of course topology changes would lead to different numerical results. For example increasing the number of feeding substations would lead to increase the loadability of the substransmission system. However, topology changes do not change the general conclusions given in this paper.

The base-case network does not contain distributed generation. The voltage profile for the network with no DERs is depicted in Fig. 8. Observe that voltages are all around 1 p.u. and that there is no voltage problem. This has to be expected as we assume that the network was properly compensated before DER penetration. Compensation is obtained through a static condenser at bus 12 and proper values of tap ratios of 33 kV / 11 kV transformers. These are the transformers that connect buses 1-29, 2-30, 3-31, 4-31, 5-32, 8-36, 9-35, 10-33, 11-34, 27-37 and 28-37 (for the sake of simplicity, we assume that the tap ratio of these transformers is fixed). The compensation allows sustaining voltage levels at the 11 kV rate buses although the power flow is from the 33 kV area to the 11 kV one.

For remedial actions an ULTC and SVCs are considered along with local DER voltage regulation.

The ULTC is placed at line 40-39, so that voltage of the feeding substation can be varied according to the loading level of the distribution system. To be more effective, the ULTC controls a remote bus within the distribution network. This bus has been selected

using a sensitivity analysis of the power flow solution at the base case loading condition as described in (Morison et al. 1993). Based on this sensitivity analysis, the weakest bus is bus 29 (participation factor $p_{ij} = 0.1207$ to the lowest power flow Jacobian eigenvalue $\mu_i = 0.06981$), while the second weakest bus is bus 37 (participation factor $p_{ij} = 0.2329$ to the second lowest power flow Jacobian eigenvalue $\mu_i = 0.16724$). Other methods can be used to select the regulated buses (see for example the methodologies proposed in (Conejo and Aguilar 1998) and (Conejo et al. 1993)), but this is beyond the scope of this paper. The technique proposed in (Morison et al. 1993) is used in this paper because it is reasonably simple and accurate. The sensitivity analysis of (Morison et al. 1993) is also used to select the buses where to place SVC devices. In particular, two SVCs are placed at buses 29 and 37. The number of SVCs as well as their size can be different. However, the main conclusion drawn with the given SVC configuration and other configurations would be similar. Note that in this paper we are not looking for the *best* remedial action, but studying the effect of several reasonable *good* solutions to maintain voltage stability on a distribution network with DERs.

For time domain simulations, a wind ramp of about 15 seconds has been used (see Fig. 9), starting from a DER generation parameter $\lambda = 1$ (see Table 2 in the Appendix). The wind model is a composite model which contains a ramp, a gust component, and a turbulence component (Slootweg 2003). Observe that the wind ramp, although realistic, is severe, thus forcing the network to face voltage instability if proper remedial actions are not considered.

Constant Power Factor

If each wind generator operates maintaining the power factor of its feeding bus close to one (i.e., 1.0), the resulting voltage profile in bus 6 as the amount of energy produced by DERs increases is depicted in Fig. 10. For this simulation the voltage at the feeding substation is 1.0 p.u., which is a reasonable value for a DER generation factor $\lambda = 1$. However, if the DER generation decreases or increases, the voltage level in the distribution network decreases. Observe that the upper (stable) part of nose curve depicted in Fig. 10 is not monotonically decreasing, as it is usual in CPF analysis. For low values of the DER generation factor λ, bus voltages are low because the feeding substation is not able to provide the adequate amount of reactive power; while for high values of λ, bus voltages are low because the power flow from the feeding substation eventually reverts its direction. This is illustrated in Fig. 11. Finally, for a DER generation factor $\lambda \approx 2$, the system faces very low voltages and a voltage collapse eventually occurs.

The time domain evolution of the voltage at bus 6 is illustrated in Fig. 12. The system begins with a DER generation parameter $\lambda = 1$. Due to the wind power increase and the lack of voltage regulation at DER buses, voltages in the distribution network decrease as the DER generation increases. This behavior was predicted by the CPF analysis (see Fig. 10). Due to the DER dynamic model and regulation, the system reaches a final equilibrium point characterized by very low voltages (well below 0.9 p.u.). This voltage profile is not acceptable and would lead to relay line tripping and likely to voltage collapse, thus confirming the static analysis obtained by means of the CPF technique.

Voltage Control Through ULTC

Figure 13 illustrates the voltage profiles at bus 6 for several values of the voltage level at the feeding substation. Observe that the value of the feeding substation voltage can be varied to optimize the voltage level in the distribution network. Furthermore the maximum total DER generation level can be increased by means of a voltage level increase at the feeding substation.

The regulation of the voltage at the feeding substation can be easily obtained by means of an ULTC on line 40-39. To be more effective the ULTC obtains a remote measure of a *weak* bus within the distribution network, namely bus 29, and controls the voltage level of bus 39 through the tap ratio variation.

The time domain evolution of the voltage at bus 6 for the operation mode with ULTC and constant DER power factors is illustrated in Fig. 14. Observe that the final value of the voltage level is acceptable. However, the ULTC time constant is slow with respect to the wind variation (see the time evolution of the ULTC tap ratio m illustrated in Fig. 15). Observe that the time response of the ULTC is adequate for slow load variations within the distribution network. Thus the voltage level of the system is very low during the transient and can lead to relay tripping and, in turn, to voltage instability.

Constant Voltage

If each wind generator operates maintaining the voltage magnitude of its feeding bus close to a pre-specified value (e.g., 1.0), the resulting voltage profiles in bus 6 as the amount of energy produced by DERs increases is depicted in Fig. 16. The voltage profile at DER buses is constant until the maximum reactive power limit is reached. Then, the reactive power is fixed at the DER limit and the voltage decreases. As a result of the

reactive power available locally at DER buses, the total DER generation level can increase considerably with respect to the case of constant power factor operation mode.

The time domain evolution of the voltage at bus 6 for the operation mode with voltage regulation at DER buses is illustrated in Fig. 17. The final value of the voltage level is acceptable, and the time response of the DER voltage control loop is able to follow the wind evolution. Observe that the voltage has a small drop which corresponds to the saturation of the rotor current i_{dr}, as illustrated in Fig. 18.

Voltage Control Through SVCs

If each wind generator operates in a coordinated manner to maintain appropriate distributed reactive power margins and adequate voltage profile using several SVCs, the resulting voltage profiles in bus 6 as the amount of energy produced by DERs increases is depicted in Fig. 19. In particular, two SVCs have been placed at buses 29 and 37. Each SVC has a total nominal reactive power capacity of 1.5 MVAr.

The voltage profile at DER buses is constant until the maximum reactive power limit is reached. Then, the reactive power is fixed at the DER limit and the voltage decreases. In addition to reactive powers provided by DERs, the SVCs also contribute clearly to maintain the desired voltage level in the distribution network. As matter of fact, the maximum DER generation level is considerably greater than in the case of constant voltage operation mode (compare Figs. 19 and 16).

The time domain evolution of the voltage at bus 6 for the operation mode with voltage regulation at DER buses and two SVCs is illustrated in Fig. 20. The final value of the voltage level is practically unchanged with respect to the initial value, and the time response of both the DER voltage control loop and SVCs are able to follow the wind

evolution. Observe that the voltage has a small drop which correspond to the saturation of the rotor current i_{dr}. Finally, for the sake of completeness, Fig. 21 illustrates the behavior of SVC regulated susceptances. Observe that increasing the size of the SVC would not result in a DER generation increase, since SVC susceptances do not saturate.

Economic Appraisal

From the analysis in the previous case studies, it becomes apparent that a distribution network exhibiting appropriate voltage behavior might suffer severe voltage disruption if sufficient DERs are connected to it without installing appropriate reactive power sources and implementing adequate control schemes.

It can be concluded that the main responsible agents for such voltage disruptions are the DERs. In a subsidiary manner, the distribution network operator is also responsible as its task is to maintain the distribution network in good operating conditions. Loads being fed by the distribution network should bear no responsibility.

Therefore, the economic burden of the required reactive power sources and control devices should be mainly born by the DERs operating in the distribution network, although the distribution network operator should share that burden if the operating capabilities of the network becomes enhanced. Demands throughout the distribution network should not bear any economic burden.

CONCLUSIONS

Embedding DERs within weak distribution networks enables increasing supply reliability, a more secure network operation (as a result of decentralization) and generally smaller supply costs. However, voltage disruption due to inappropriate reactive power availability might occur as the substation-to-load flows decrease and eventually revert

directions. Non-free remedial actions are needed to maintain both an appropriate voltage profile and an appropriate voltage stability margin. Conventional ULTC devices that provide adequate steady state voltage support might not behave adequately for a fast increment in DER generation. Therefore, faster control devices such as SVCs might be required. Both the distribution network operator and the DER owners should bear the economical burden of the remedial actions. The above conclusions are drawn for comprehensive case studies.

Further research work will concentrate in finding both the optimal amount and the optimal location of remedial actions based on SVC devices.

ACKNOWLEDGMENTS

The authors are partly supported by the Ministry of Science and Education of Spain through CICYT Project DPI-2003-01362 and by Junta de Comunidades de Castilla - La Mancha through project PBI-05-053.

APPENDIX I. NOTATION

This appendix provides notation and data of the DERs, the ULTC and the SVCs used in the case studies discussed in the paper.

Power flow variables and parameters

Power flow data of the test system can be found in (Greene and Dobson 1998). The notation for power flow variables and parameters is as follows:

v_i = Voltage magnitude at bus i.

θ_i = Voltage phase at bus i.

P_i = Active power injection at bus i.

Q_i = Reactive power injection at bus i.

$Y_{ik}\angle\alpha_{ik}$ = Element (i,k) of the admittance matrix.

DER variables and parameters

The list of DER variables is as follows:

$v_{ds} + jv_{qs}$ = Stator voltage.

$v_{dr} + jv_{qr}$ = Rotor voltage.

$i_{ds} + ji_{qs}$ = Stator current.

$i_{dr} + ji_{qr}$ = Rotor current.

ω_m = Rotor speed.

T_m = Mechanical Torque.

T_e = Electrical Torque.

P_w = Mechanical power extracted from the wind.

θ_p = Pitch angle.

v_t = Blade tip speed.

v_w = Wind speed.

c_p = Performance coefficient.

ξ = Tip speed ratio.

Table 2 provides static data of the DERs used for CPF analysis. The active power P_0 is the *base case* power that correspond to the DER generation parameter $\lambda = 1$. The voltage V_0 is the desired voltage used in the constant voltage operation mode. Table 3 provides the dynamic data used for each DER. Data includes parameters of induction generator, wind turbine, pitch control, voltage control and power control.

ULTC variables and parameters

The list of ULTC variables is as follows:

m = Tap ratio.

Table 4 provides dynamic data of the ULTC placed on line 40-39.

SVC variables and parameters

The list of SVC variables is as follows:

b_{SVC} = SVC total susceptance.

Table 5 provides dynamic data of the SVCs placed at buses 29 and 37, respectively. The size of each SVCs is 1.5 MVAr. Maximum and minimum susceptances are in p.u. on SVC ratings.

REFERENCES

B.O.E. 219 (1985). "Administrative and Technical Standards for Operation and Connection to the Electric Grid of Power Plants up to 5000 kVA, and Electrical Self-Generation (in Spanish)." *Report No. 219*, Ministerio de Industria y Energía.

Cañizares, C. A. (2002). "Voltage Stability Assessment: Concepts, Practices and Tools." *Report No. SP101PSS*, IEEE/PES Power System Stability Subcommittee, Final Document. Available at http://www.power.uwaterloo.ca.

Cano-Marín, R., Gómez-Expósito, A., and Burgos-Payán, M. (2004). "Wind Energy Integration in Distribution Networks: A Voltage-Stability Constrained Case Study." *Proceedings of the VI Bulk Power System Dynamics and Control*, Cortina d'Ampezzo, Italy.

Conejo, A. J. and Aguilar, M. J. (1998). "Secondary Voltage Control: Nonlinear Selection of Pilot Buses, Design of an Optimal Control Law, and Simulation Results." *IEE Proceedings - Generation, Transmission and Distribution*, 145(1), 77–81.

Conejo, A. J., Gómez, T., and de la Fuente, J. I. (1993). "Pilot Bus Selection for Secondary Voltage Control." *European Transactions on Electric Power Engineering*, 3(5), 359–366.

DeMeo, E., Grant, W., Milligan, M. R., and Schuerger, M. J. (2005). "Wind Plant Integration: Costs, Status, and Issues." *IEEE Power & Energy Magazine*, 38–46.

Eriksen, P. B., Ackerman, T., Abildgaard, H., Smith, P., Winter, W., and Rodríguez-García, J. (2005). "System Operation with High Wind Penetration: The Challenges of Denmark, Germany, Spain, and Ireland." *IEEE Power & Energy Magazine*, 65–74.

EWEA (2005). "Wind Force 12-A. Blueprint to Achive 12% of the World's Electricity from Wind Power by 2020." *Report No. 2005*, European Wind Energy Association. available at www.ewea.org.

Fan, J. and Salman, S. K. (1997). "The Effect of Integration of Wind Farms into Utility Network on Voltage Control due to the Co-ordination of AVC Relays." *Proceedings of the Fourth International Conference on Advances in Power System Control, Operation and Management, APSOM-97*, Vol. 1.

Fengquan, Z., Joos, G., and Abbey, C. (2005). "Voltage Stability in Weak Connection Wind Farms." *Proceedings of the IEEE Power Engineering Society General Meeting*, San Francisco, CA.

Freitas, W., Vieira, J. C. M., da Silva, L. C. P., Affonso, C. M., and Morelato, A. (2005). "Long-term Voltage Stability of Distribution Systems With Induction Generators." *Proceedings of the IEEE Power Engineering Society General Meeting*, San Francisco,

CA.

Greene, S. and Dobson, I. (1998). "Voltage Collapse Margin Sensitivity Methods applied to the Power System of Southwest England. Available at http://www.pserc.wisc.edu.

Ha, L. T. and Saha, T. K. (2004). "Investigation of Power Loss and Voltage Stability Limits for Large Wind Farm Connections to a Subtransmission Network." *Proceedings of the IEEE Power Engineering Society General Meeting*, Denver, CO.

Hatziargyriou, N. D., Karakatsanis, T. S., and Papadopoulos, M. P. (1997). "The Effect of Wind Parks on the Operation of Voltage Control Devices." *Proceedings of the 14th International Conference and Exhibition on Electricity Distribution. Part 1. Contributions*, Vol. 5.

Hawkins, N. T. (1996). "On-line Reactive Power Management in Electric Power Systems," PhD thesis, University of London.

Milano, F. (2002). "PSAT, Matlab-based Power System Analysis Toolbox. Available at http://thundebox.uwaterloo.ca/∼fmilano.

Milano, F. (2005). "An Open Source Power System Analysis Toolbox." *IEEE Transactions on Power Systems*, 20(3), 1199–1206.

Miller, A., Muljadi, E., and Zinger, D. S. (1997). "A Variable Speed Wind Turbine Power Control." *IEEE Transactions on Energy Conversion*, 12(2), 181–186.

Morison, G. K., Gao, B., and Kundur, P. (1993). "Voltage Stability Analysis using Static and Dynamic Approaches." *IEEE Transactions on Power Systems*, 8(3), 1159–1171.

Muljadi, E. and Butterfield, C. P. (2001). "Pitch-controlled Variable-speed Wind Turbine Generation." *IEEE Transactions on Industry Applications*, 37(1), 240–246.

Pálsson, M. T., Toftvaag, T., Uhlen, K., and Tande, J. O. G. (2002). "Large-scale Wind

Power Integration and Voltage Stability Limits in Regional Networks." *Proceedings of the IEEE Power Engineering Society General Meeting*, Chicago, IL.

Pálsson, M. T., Toftvaag, T., Uhlen, K., and Tande, J. O. G. (2003). "Control Concepts to Enable Increased Wind Power Penetration." *Proceedings of the IEEE Power Engineering Society General Meeting*, Toronto, Canada.

Pool, R. (2005). "Scaling New Heights. The Trials and Tribulations of Building an Offshore Wind Farm." *IEE Power Engineer*, 20–23.

Slootweg, J. G. (2003). "Wind Power: Modelling and Impact on Power System Dynamics," PhD thesis, Delft University of Technology.

Slootweg, J. G., de Haan, S. W. H., Polinder, H., and Kling, W. L. (2003). "General Model for representing Variable Speed Wind Turbines in Power System Dynamics Simulations." *IEEE Transactions on Power Systems*, 18(1), 144–151.

Slootweg, J. G., Polinder, H., and Kling, W. L. (2005). "Representing Wind Turbine Electrical Generating Systems in Fundamental Frequency Simulations." *IEEE Transactions on Power Systems*, 20(3), 1199–1206.

Tapia, A., Tapia, G., Ostolaza, J. X., Saenz, J. R., Criado, R., and Berasategui, J. L. (2001). "Reactive Power Control of a Wind Farm Made up with Doubly Fed Induction Generators." *Proceedings of the IEEE Porto Power Tech Conference*, Porto, Portugal.

Zavadil, R., Miller, N., Ellis, A., and Muljadi, E. (2005). "Making Connections: Wind Generation Challenges and Progress." *IEEE Power & Energy Magazine*, 26–37.

List of Tables

1 DER Operation Modes. 31

2 Static Data of DERs 32

3 Dynamic Data of DERs 33

4 ULTC Data 34

5 SVC Data 35

List of Figures

1 Rotor speed control scheme. 36

2 Voltage control scheme. 37

3 Power-speed characteristic. 38

4 Pitch angle control scheme. 39

5 Under Load Tap Changer: remote voltage control. 40

6 SVC regulator scheme. 41

7 40-bus test system. 42

8 Voltage profile without wind generation for $v_{\text{Bus }40} = 1.05$ p.u. at the interconnection bus. 43

9 Wind speed ramp used for time domain simulations. 44

10 Constant power factor: Voltage profile at bus 6 as a function of the DER generation parameter λ. 45

11 Constant power factor: Active and reactive powers provided by the feeding substation at bus 40 as a function of the DER generation parameter λ. Powers are in p.u. on a 100 MVA base. 46

12 Constant power factor: Voltage profile at bus 6 for the 40-bus network with wind ramp. 47

13 ULTC Control: Voltage profiles at bus 6 as a function of the DER generation parameter λ and parametrized with respect to the interconnection bus voltage $v_{\text{Bus }40}$. 48

14 ULTC Control: Voltage profile at bus 6 for the 40-bus network with wind ramp and one ULTC at line 40-39 and remote voltage control at bus 29. . . 49

15 ULTC Control: Tap ratio of the ULTC at line 40-39 and remote voltage control at bus 29. 50

16 Constant voltage: Voltage profiles at bus 6 as a function of the DER generation parameter λ with regulated voltages at DERs. 51

17 Constant voltage: Voltage profiles at bus 6 for the 40-bus network with wind ramp and regulated voltages at DERs. 52

18 Constant voltage: Current i_{dr} of wind turbine at bus 6 for the 40-bus network with wind ramp and regulated voltages at DERs. 53

19 SVC control: Voltage profiles at bus 6 as a function of the DER generation parameter λ with regulated voltages at DERs and 2 SVCs at buses 29 and 37. 54

20 SVC control: Voltage profiles at bus 6 for the 40-bus network with wind ramp, regulated voltages at DERs and 2 SVCs at buses 29 and 37. 55

21 SVC control: Susceptances of SVCs at buses 29 and 37. Susceptances are in p.u. on 100 MVA and 11 kV bases. 56

TABLE 1. DER Operation Modes.

Control Type	Case 1	Case 2	Case 3	Case 4
Constant Power Factor	✓	✓		
ULTC Voltage Control		✓		
Constant DER Voltages			✓	✓
SVC Voltage Control				✓

TABLE 2. Static Data of DERs

Bus	P_0 MW	V_0 p.u.	$Q^{\max}$ MVAr	$Q^{\min}$ MVAr
6	4.8468	1.02	2.4	-2.4
13	2.7775	1.01	1.4	-1.4
18	5.4955	1.02	2.75	-2.75
20	1.039	1	0.5	-0.5
22	1.039	1	0.5	-0.5
24	2.895	1.005	1.4	-1.4
39	6.1875	0.996	3.0	-3.0

TABLE 3. Dynamic Data of DERs

Variable	Description	Unit	Value
S_n	Power rating	MVA	20
V_n	Voltage rating	kV	33 - 11
f_n	Frequency rating	Hz	50
r_S	Stator resistance	p.u.	0.01
x_S	Stator reactance	p.u.	0.1
r_R	Rotor resistance	p.u.	0.01
x_R	Rotor reactance	p.u.	0.08
x_m	Magnetizing reactance	p.u.	3
H_m	Rotor inertia	kWs/kVA	3
K_p	Pitch control gain	-	1000
T_p	Pitch control time constant	s	3
K_V	Voltage control gain	-	10.00
T_ϵ	Power control time constant	s	0.01
R	Rotor radius	m	75
p	Number of poles	int	4
n_b	Number of blades	int	3
η_{GB}	Gear box ratio	-	0.011236

TABLE 4. ULTC Data

Variable	Description	Unit	Value
-	Bus k (from)	int	40
-	Bus m (to)	int	39
S_n	Power rating	MVA	100
V_n	Voltage rating	kV	132
f_n	Frequency rating	Hz	50
k_T	Nominal tap ratio	kV/kV	132/33
H	Integral deviation	p.u.	0.001
K	Inverse time constant	1/s	0.1
$m_{\max}$	Max tap ratio	p.u./p.u.	1.15
$m_{\min}$	Min tap ratio	p.u./p.u.	0.85
V_{ref}	Reference voltage	p.u.	1.08
x_T	Transformer reactance	p.u.	0.006375
r_T	Transformer resistance	p.u.	0.000108
r	Bus r (remote voltage control)	int	29

TABLE 5. SVC Data

Variable	Description	Unit	Value
-	Bus number	int	(29, 37)
S_n	Power rating	MVA	1.5
V_n	Voltage rating	kV	11
f_n	Frequency rating	Hz	50
T_r	Regulator time constant	s	10
K_r	Regulator gain	-	100
V_{ref}	Reference Voltage	p.u.	1
$b_{\max}$	Maximum susceptance	p.u.	1
$b_{\min}$	Minimum susceptance	p.u.	-1

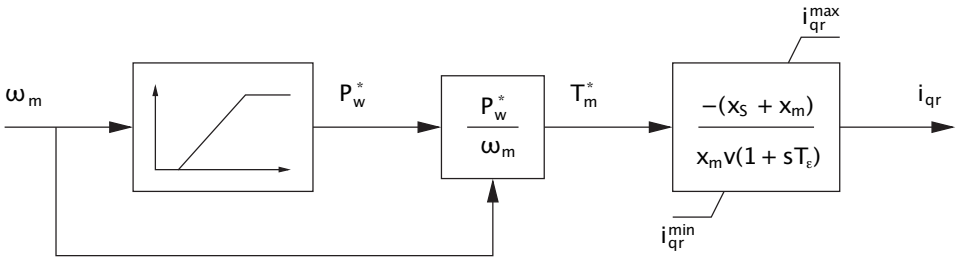

FIG. 1. Rotor speed control scheme.

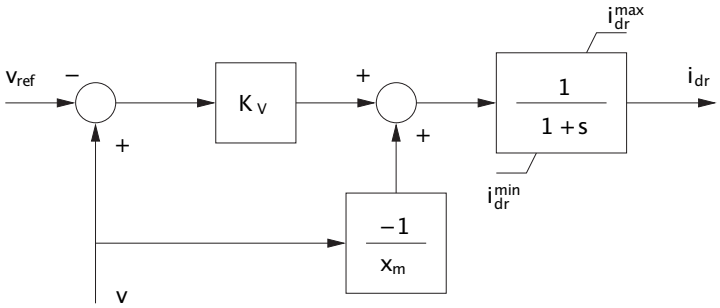

FIG. 2. Voltage control scheme.

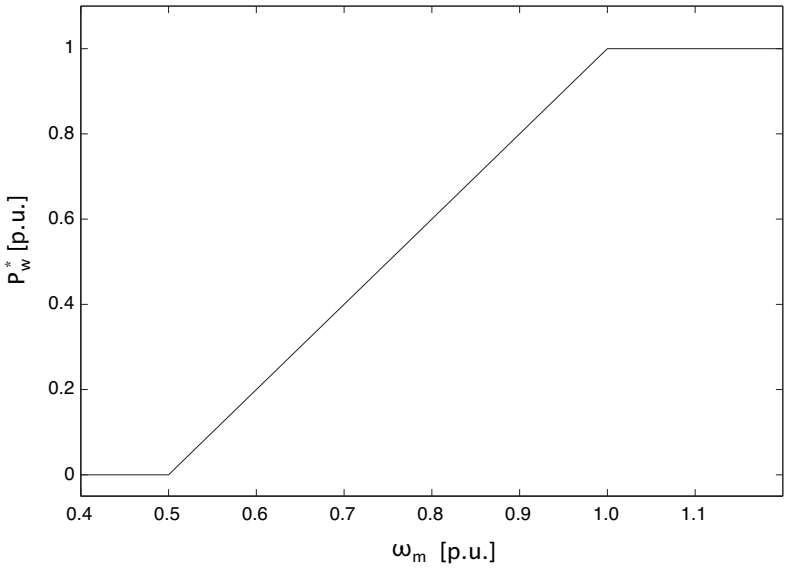

FIG. 3. Power-speed characteristic.

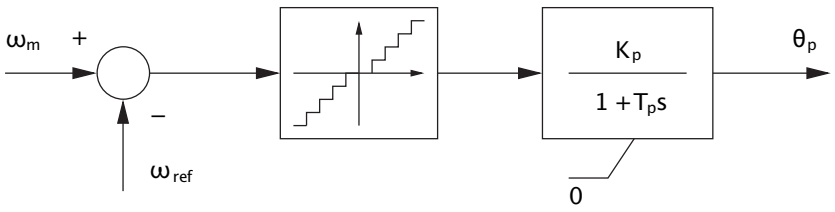

FIG. 4. Pitch angle control scheme.

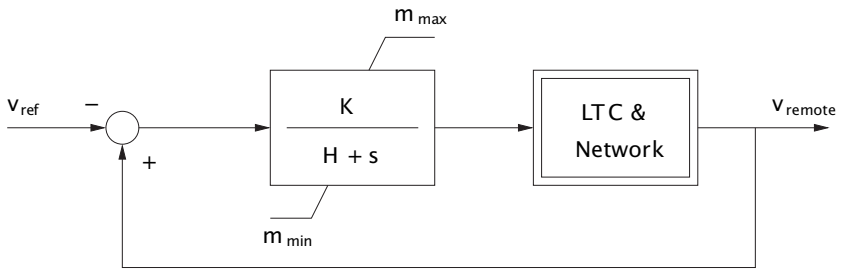

FIG. 5. Under Load Tap Changer: remote voltage control.

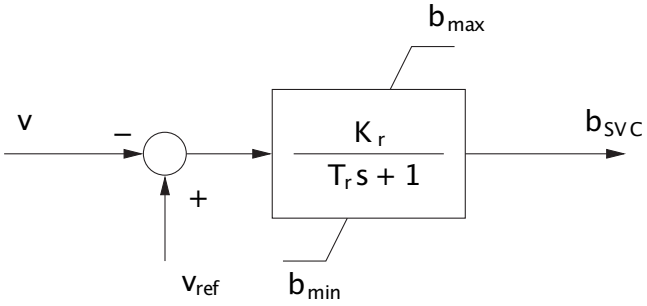

FIG. 6. SVC regulator scheme.

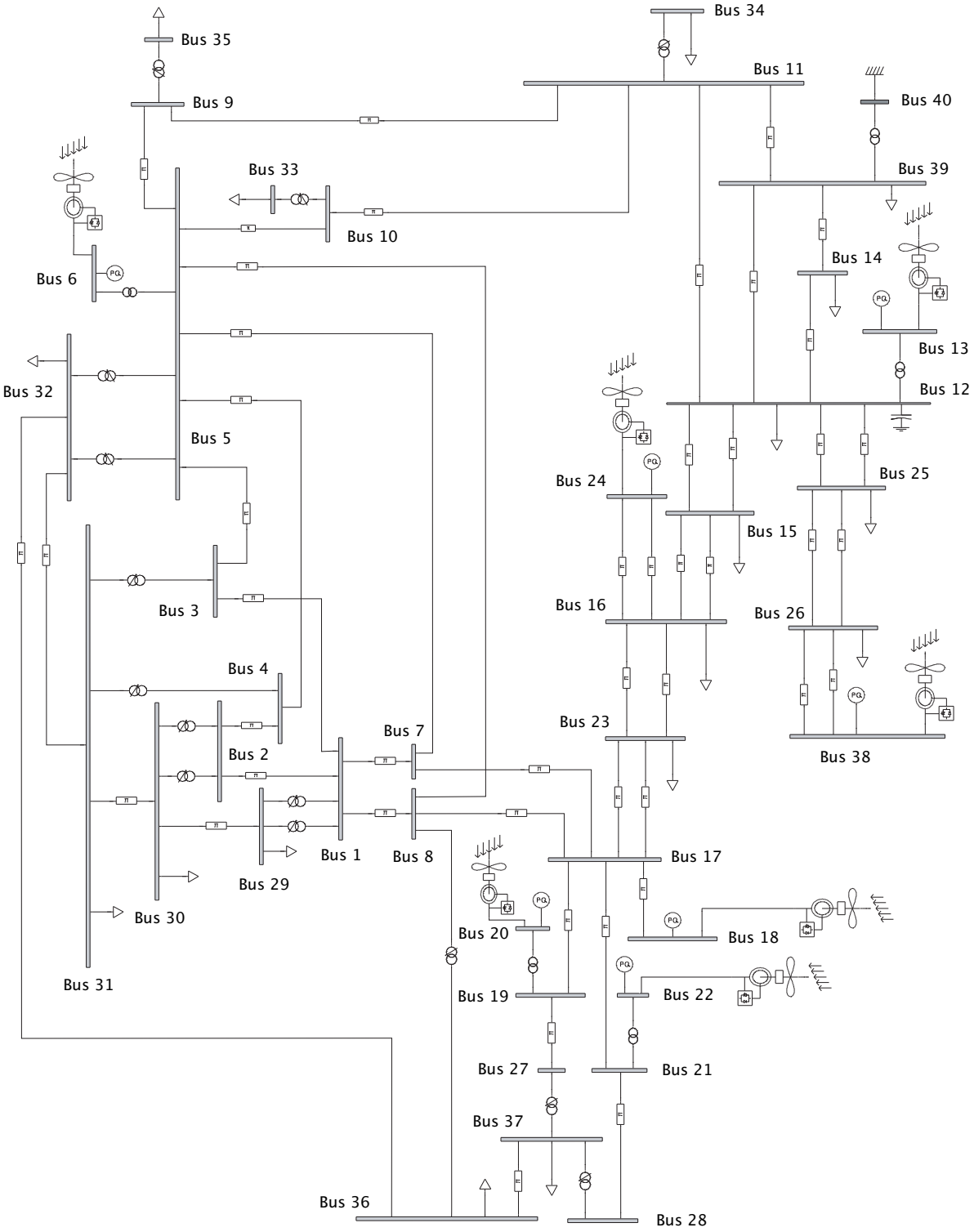

FIG. 7. 40-bus test system.

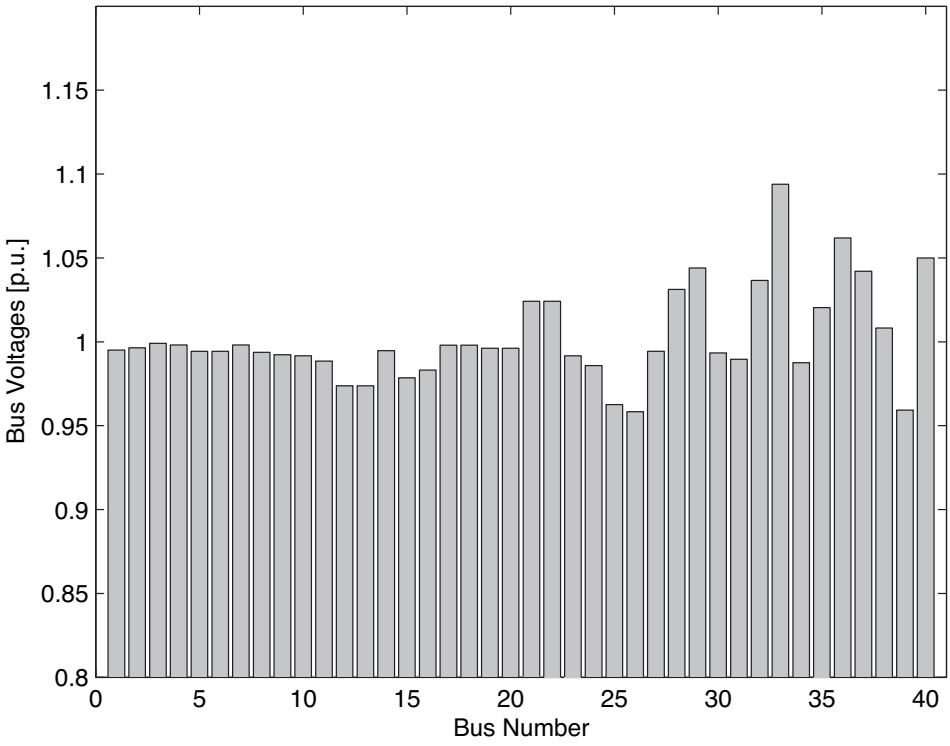

FIG. 8. Voltage profile without wind generation for $v_{\text{Bus 40}} = 1.05$ p.u. at the interconnection bus.

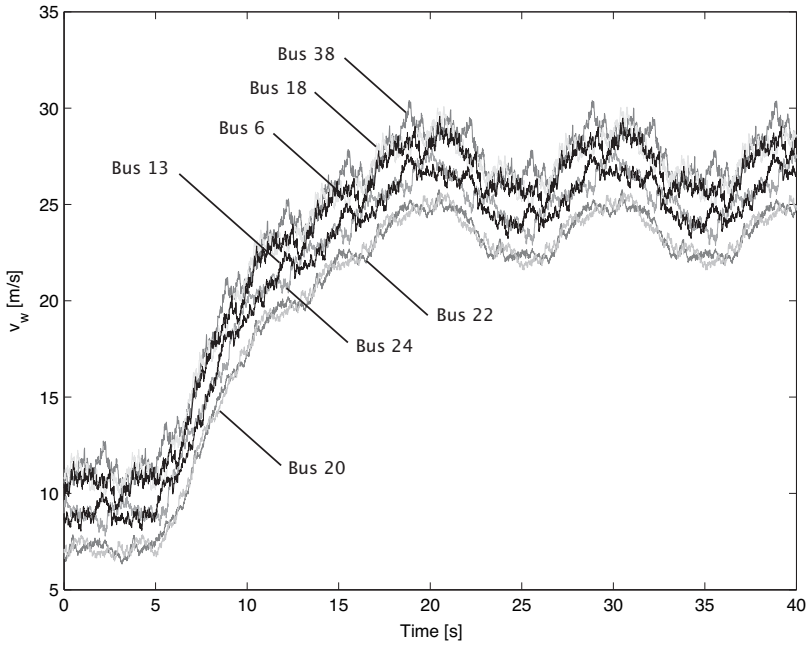

FIG. 9. Wind speed ramp used for time domain simulations.

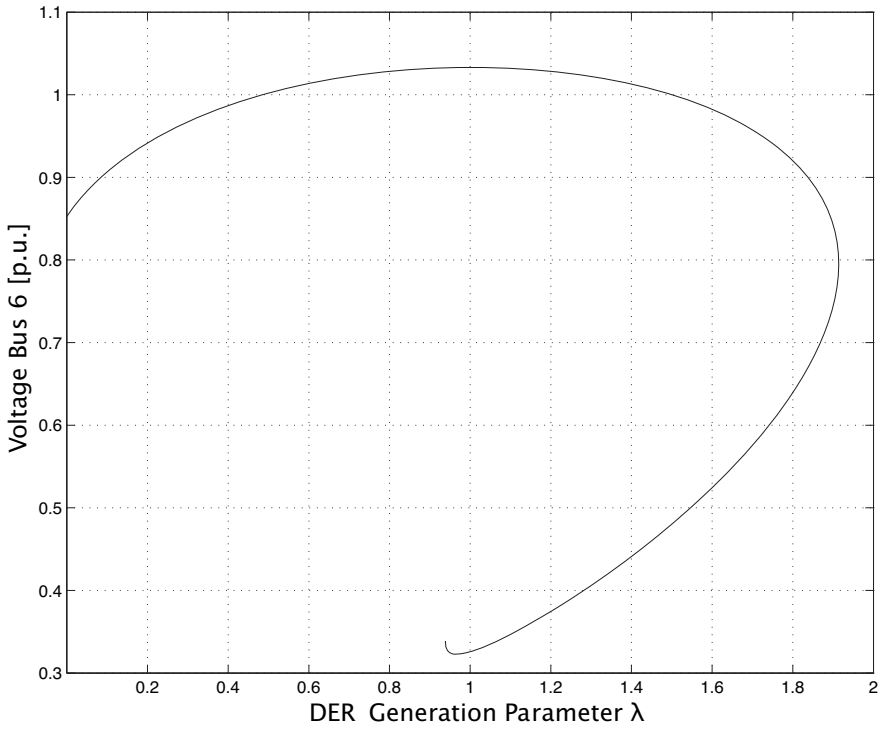

FIG. 10. Constant power factor: Voltage profile at bus 6 as a function of the DER generation parameter λ.

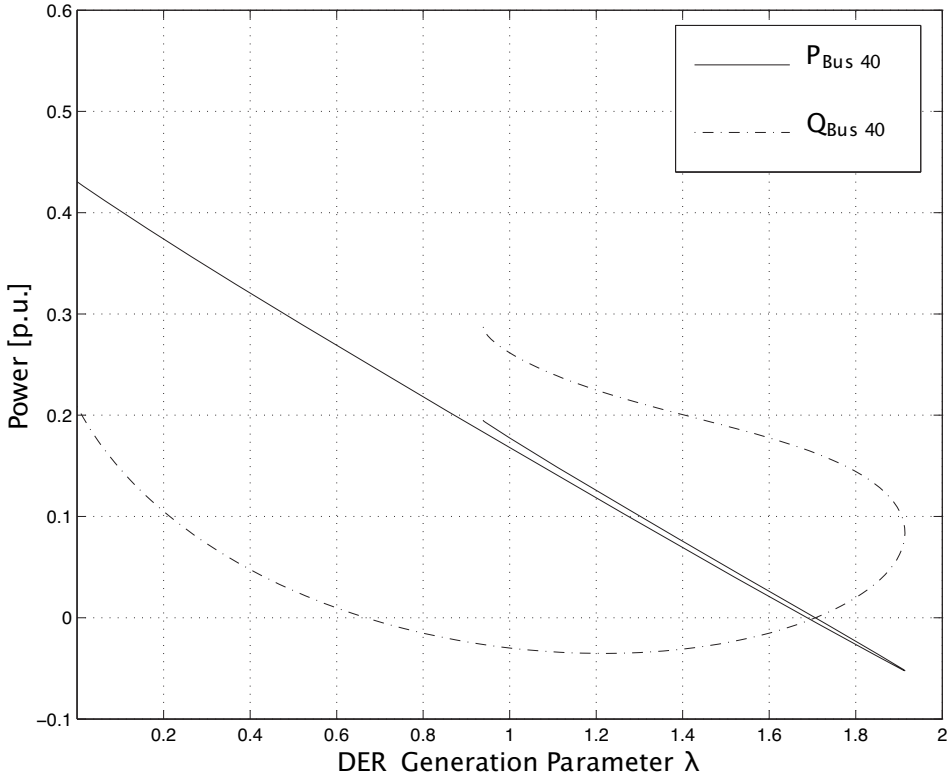

FIG. 11. Constant power factor: Active and reactive powers provided by the feeding substation at bus 40 as a function of the DER generation parameter λ. Powers are in p.u. on a 100 MVA base.

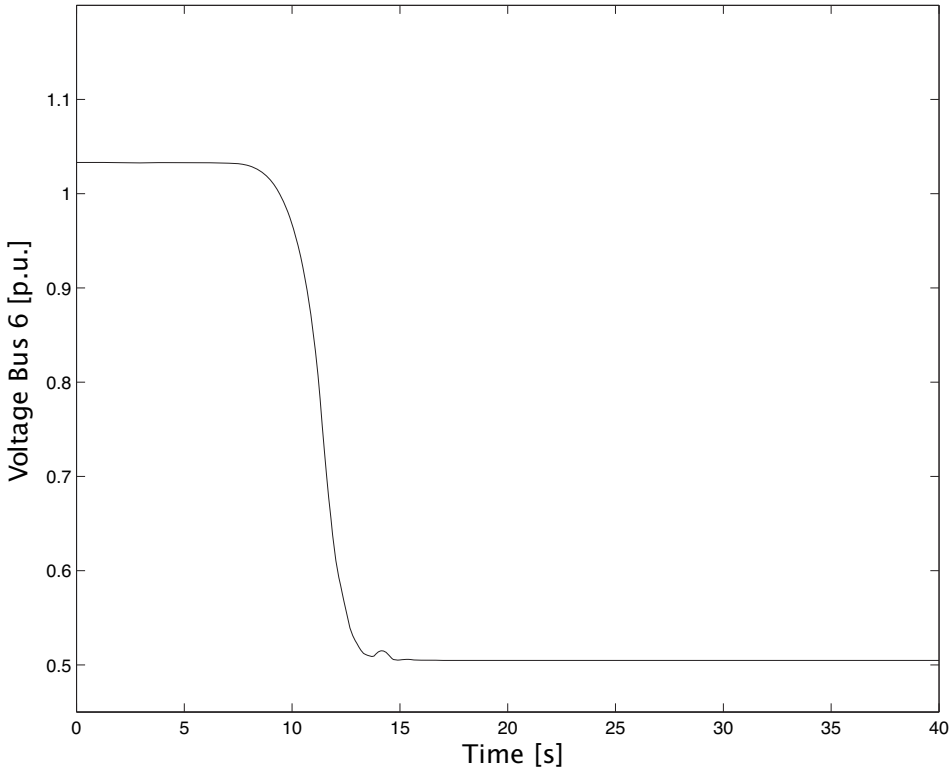

FIG. 12. Constant power factor: Voltage profile at bus 6 for the 40-bus network with wind ramp.

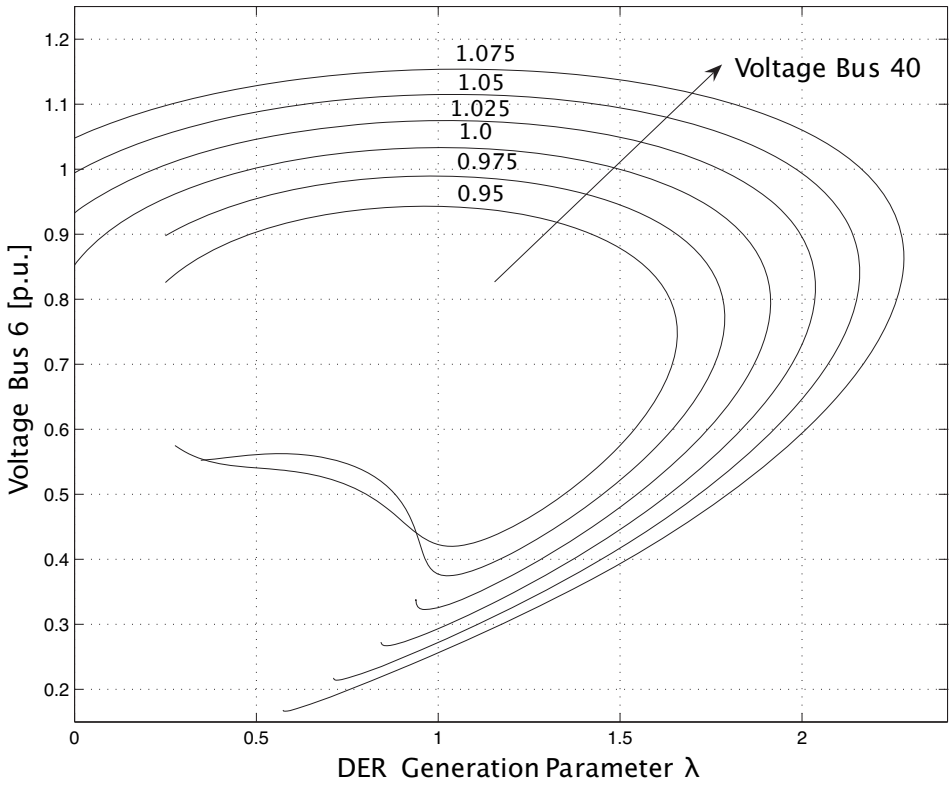

FIG. 13. ULTC Control: Voltage profiles at bus 6 as a function of the DER generation parameter λ and parametrized with respect to the interconnection bus voltage $v_{\text{Bus 40}}$.

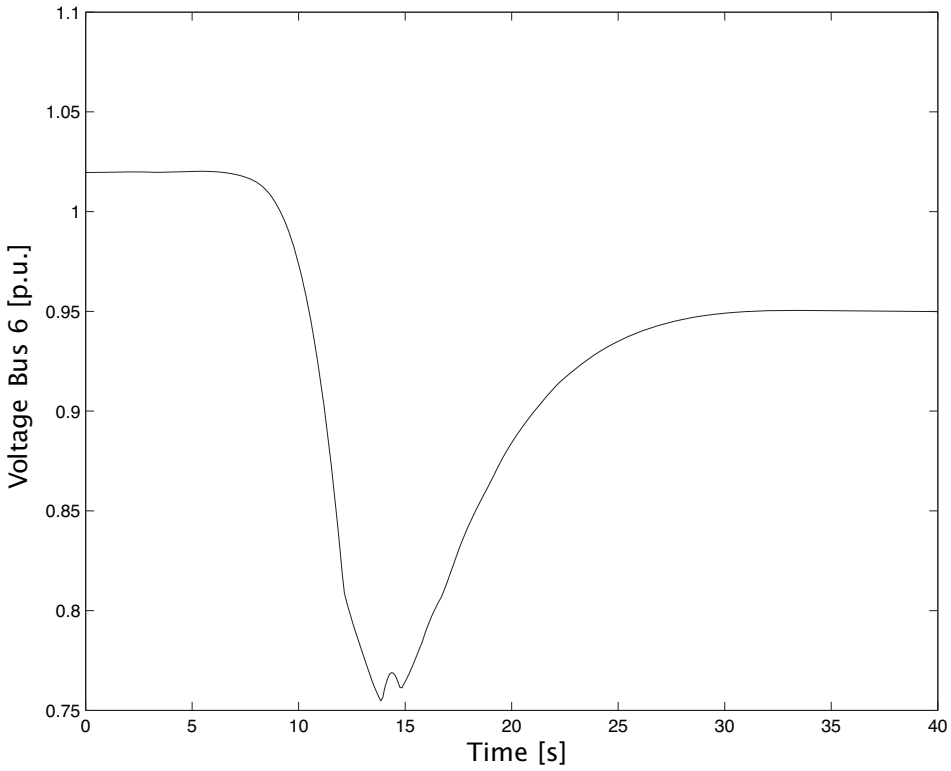

FIG. 14. ULTC Control: Voltage profile at bus 6 for the 40-bus network with wind ramp and one ULTC at line 40-39 and remote voltage control at bus 29.

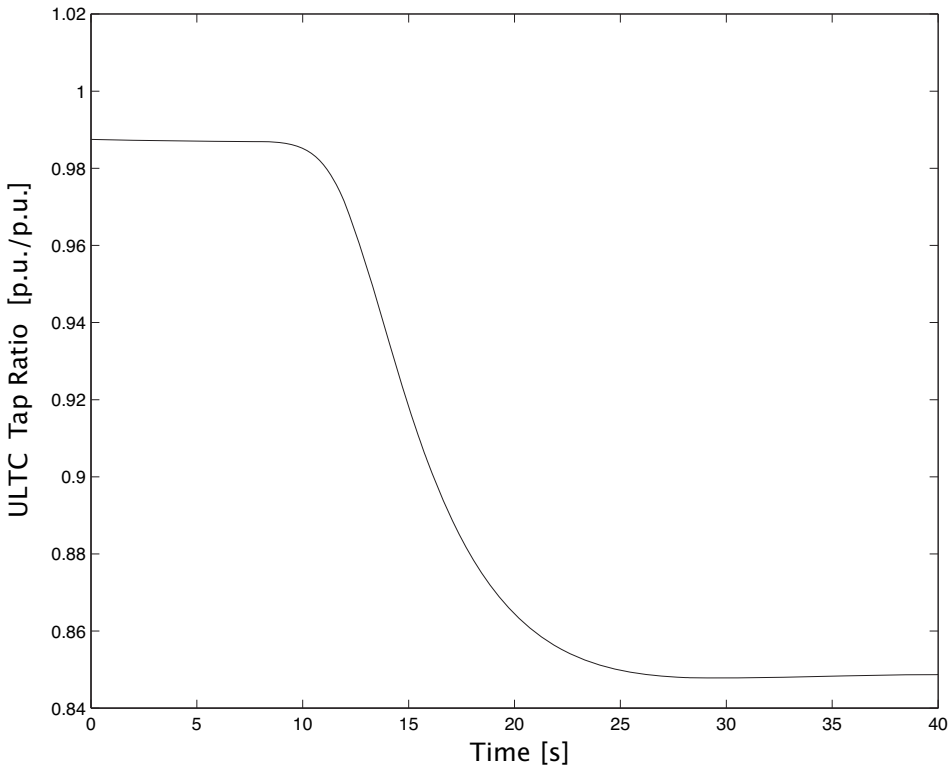

FIG. 15. ULTC Control: Tap ratio of the ULTC at line 40-39 and remote voltage control at bus 29.

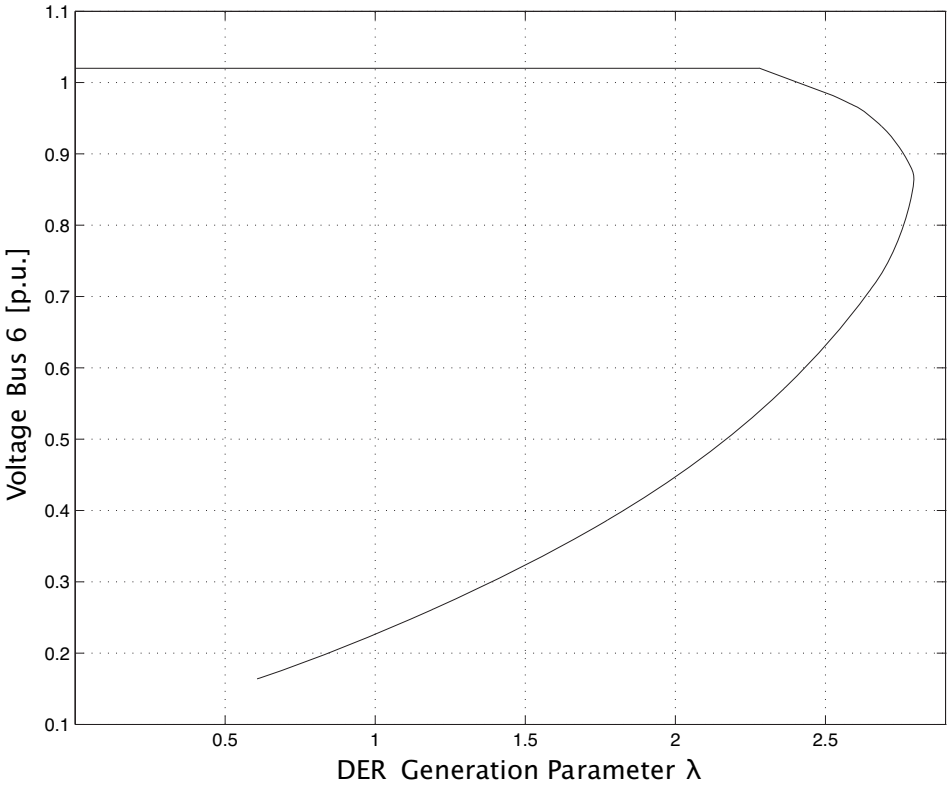

FIG. 16. Constant voltage: Voltage profiles at bus 6 as a function of the DER generation parameter λ with regulated voltages at DERs.

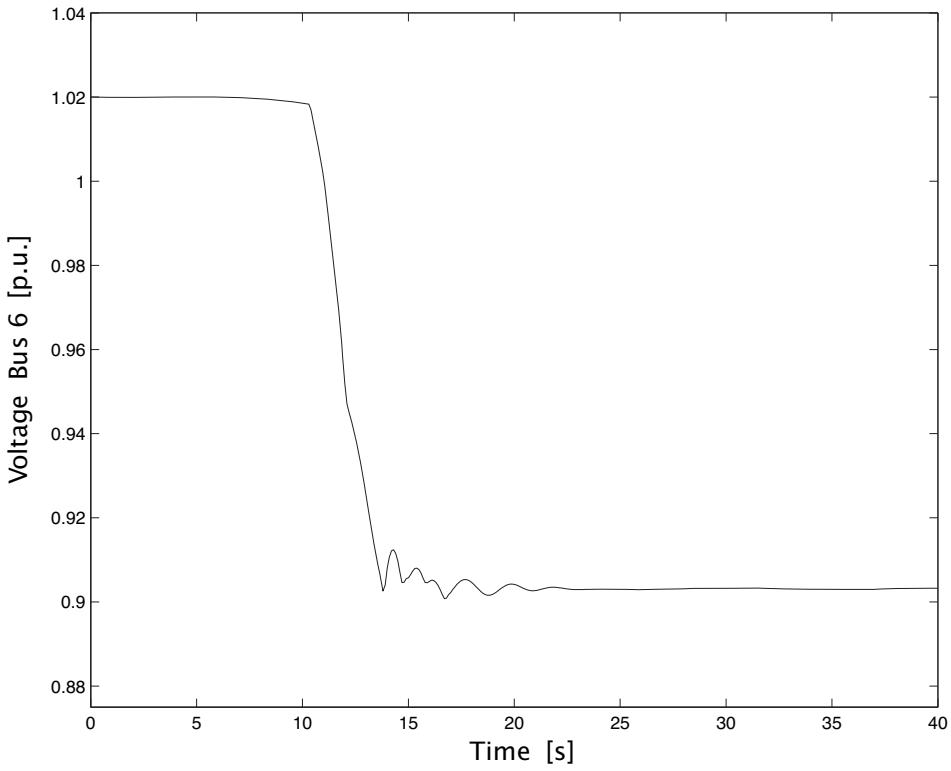

FIG. 17. Constant voltage: Voltage profiles at bus 6 for the 40-bus network with wind ramp and regulated voltages at DERs.

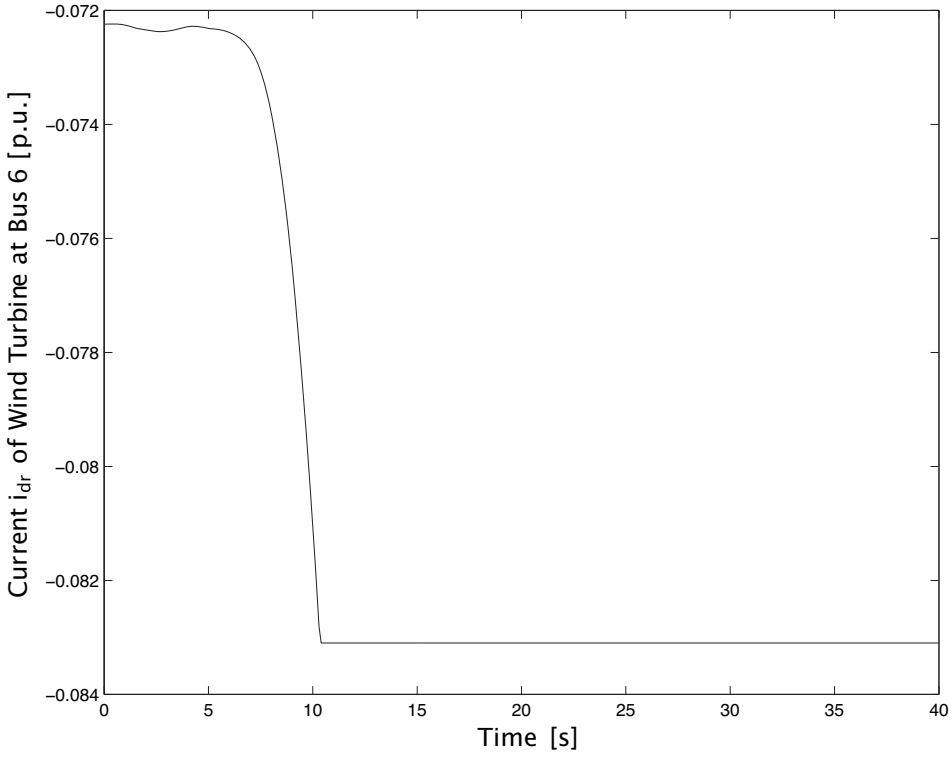

FIG. 18. Constant voltage: Current i_{dr} of wind turbine at bus 6 for the 40-bus network with wind ramp and regulated voltages at DERs.

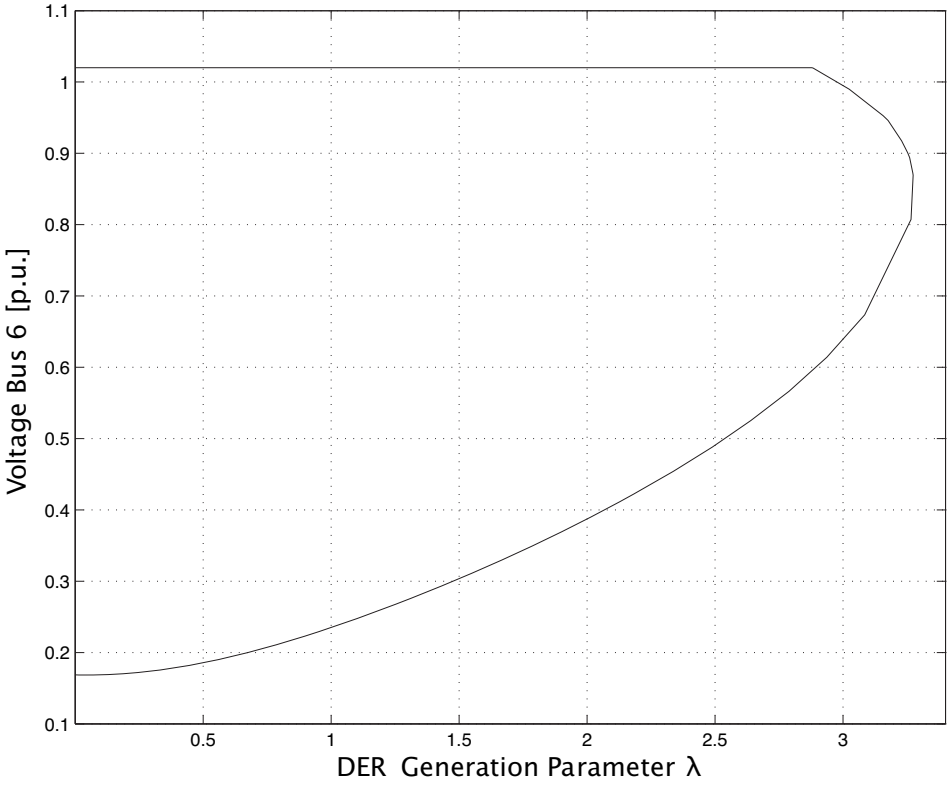

FIG. 19. SVC control: Voltage profiles at bus 6 as a function of the DER generation parameter λ with regulated voltages at DERs and 2 SVCs at buses 29 and 37.

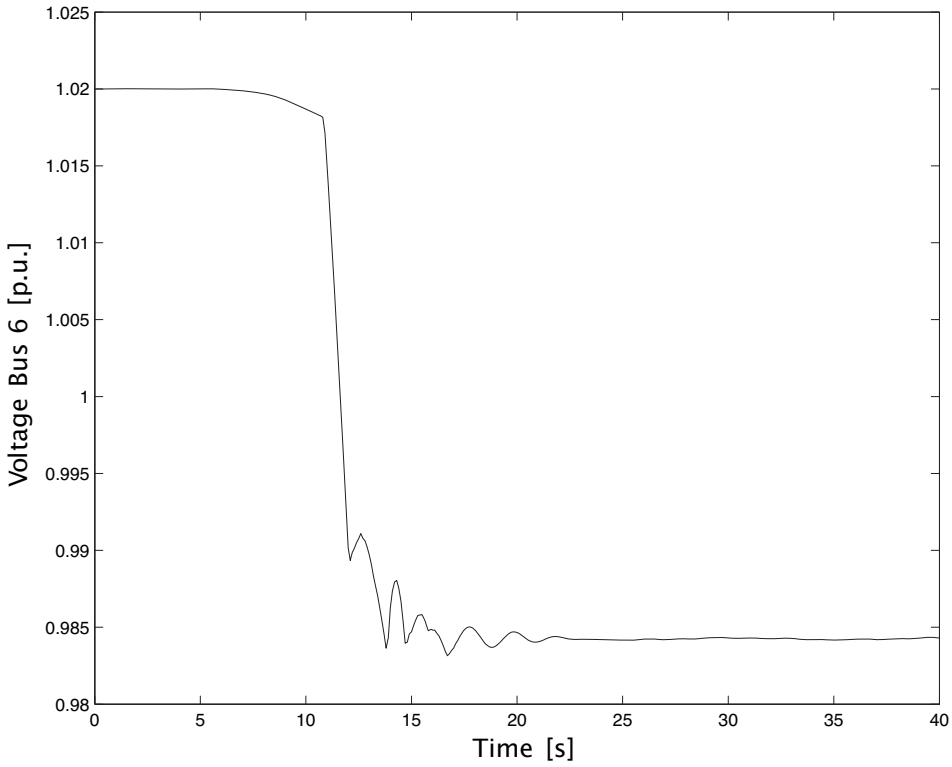

FIG. 20. SVC control: Voltage profiles at bus 6 for the 40-bus network with wind ramp, regulated voltages at DERs and 2 SVCs at buses 29 and 37.

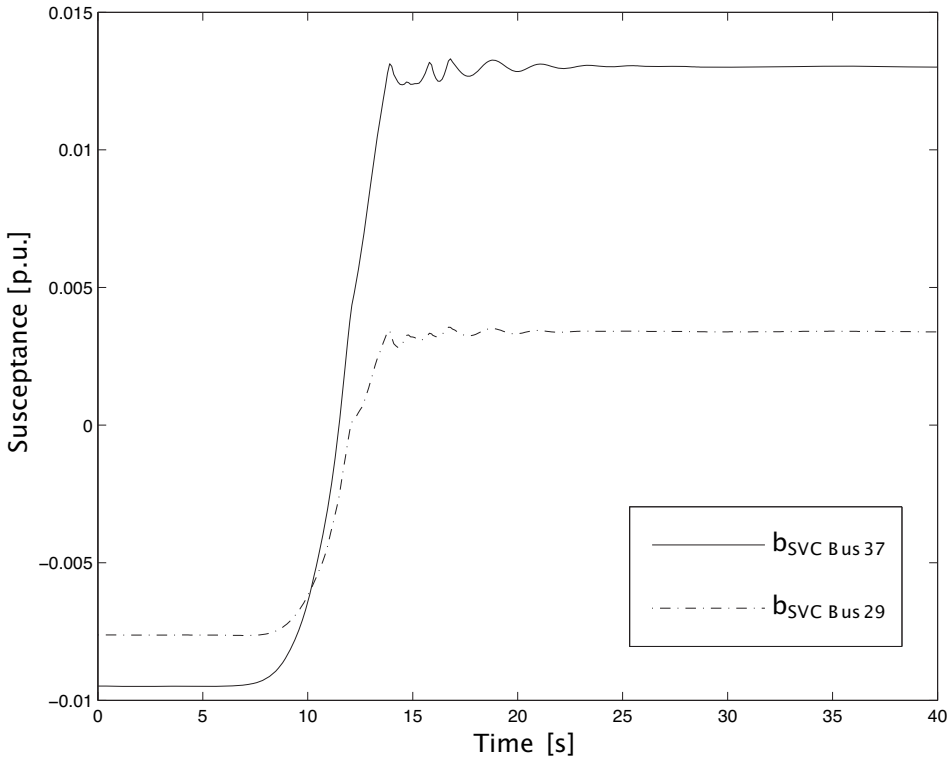

FIG. 21. SVC control: Susceptances of SVCs at buses 29 and 37. Susceptances are in p.u. on 100 MVA and 11 kV bases.